Ground-state configuration of neutron-rich ^{35}Al via Coulomb breakup

S. Chakraborty,[1] Ushasi Datta,[1,2,*] T. Aumann,[2,3] S. Beceiro-Novo,[4] K. Boretzky,[2] C. Caesar,[2] B. V. Carlson,[5] W. N. Catford,[6] M. Chartier,[7] D. Cortina-Gil,[4] G. De Angelis,[8] P. Diaz Fernandez,[4,9] H. Emling,[2] O. Ershova,[2] L. M. Fraile,[10] H. Geissel,[2,11] D. Gonzalez-Diaz,[2] H. Johansson,[9] B. Jonson,[9] N. Kalantar-Nayestanaki,[12] T. Kröll,[3] R. Krücken,[13] C. Langer,[2] T. Le Bleis,[13] Y. Leifels,[2] J. Marganiec,[2,3] G. Münzenberg,[2] M. A. Najafi,[12] T. Nilsson,[9] C. Nociforo,[2] V. Panin,[2] R. Plag,[2] A. Rahaman,[1] R. Reifarth,[2] M. V. Ricciardi,[2] C. Rigollet,[12] D. Rossi,[2] C. Scheidenberger,[2,11] H. Scheit,[3] H. Simon,[2] J. T. Taylor,[7] Y. Togano,[2] S. Typel,[2] Y. Utsuno,[14] A. Wagner,[15] F. Wamers,[2] H. Weick,[2] and J. S. Winfield[2]

[1]*Saha Institute of Nuclear Physics, Kolkata 700064, India*
[2]*GSI Helmholtzzentrum für Schwerionenforschung GmbH, D-64291 Darmstadt, Germany*
[3]*Technische Universität Darmstadt, 64289 Darmstadt, Germany*
[4]*Universidade de Santiago de Compostela, 15706 Santiago de Compostela, Spain*
[5]*Instituto Tecnologico de Aeronautica-CTA 12228-900, Sao Jose dos Campos, Brazil*
[6]*University of Surrey, Guildford GU2 5XH, United Kingdom*
[7]*University of Liverpool, Liverpool L69 7ZE, United Kingdom*
[8]*INFN, Laboratori Nazionali di Legnaro, Via Romea 4, I-35020 Legnaro, Italy*
[9]*Fundamental Fysik, Chalmers Tekniska Högskola, S-41296 Göteborg, Sweden*
[10]*Universidad Complutense de Madrid, CEI Moncloa, E-28040 Madrid, Spain*
[11]*II. Physikalisches Institut, 35392 Giessen, Germany*
[12]*KVI-CART, University of Groningen, 9747AA Groningen, The Netherlands*
[13]*Physik Department E12, Technische Universität München, 85748 Garching, Germany*
[14]*Advanced Science Research Center, Japan Atomic Energy Agency, Tokai, Ibaraki 319-1195, Japan*
[15]*Helmholtz-Zentrum Dresden-Rossendorf, D-01328 Dresden, Germany*

(Received 15 July 2017; published 1 September 2017)

The ground-state configuration of ^{35}Al has been studied via Coulomb dissociation (CD) using the LAND-FRS setup (GSI, Darmstadt) at a relativistic energy of ∼403 MeV/nucleon. The measured inclusive differential CD cross section for ^{35}Al, integrated up to 5.0 MeV relative energy between the ^{34}Al core and the neutron using a Pb target, is 78(13) mb. The exclusive measured CD cross section that populates various excited states of ^{34}Al is 29(7) mb. The differential CD cross section of $^{35}\mathrm{Al} \rightarrow {}^{34}\mathrm{Al} + n$ has been interpreted in the light of a direct breakup model, and it suggests that the possible ground-state spin and parity of ^{35}Al could be, tentatively, $1/2^+$ or $3/2^+$ or $5/2^+$. The valence neutrons, in the ground state of ^{35}Al, may occupy a combination of either $l = 3,0$ or $l = 1,2$ orbitals coupled with the ^{34}Al core in the ground and isomeric state(s), respectively. This hints of a particle-hole configuration of the neutron across the magic shell gaps at $N = 20,28$ which suggests narrowing the magic shell gap. If the $5/2^+$ is the ground-state spin-parity of ^{35}Al as suggested in the literature, then the major ground-state configuration of ^{35}Al is a combination of $^{34}\mathrm{Al(g.s.;}\,4^-) \otimes \nu_{p_{3/2}}$ and $^{34}\mathrm{Al(isomer;}\,1^+) \otimes \nu_{d_{3/2}}$ states. The result from this experiment has been compared with that from a previous knockout measurement and a calculation using the SDPF-M interaction.

DOI: 10.1103/PhysRevC.96.034301

I. INTRODUCTION

The atomic nucleus is a complex quantum many-body system. Yet, it shows simple behavior which could be explained by a mean nuclear field, containing many ingredients of the nucleon-nucleon interactions. The characteristics of the mean nuclear field are the shell gaps at magic numbers, where extra stability in the nuclei has been observed [1]. These magic numbers play a significant role in understanding the structure of nuclei in and around the β-stability line. Recently, the disappearance or modification in the shell gaps has been observed in nuclei far from stability. The reason behind this modification or disappearance of the shell gaps could be due to the NN force, which becomes more pronounced with large neutron-proton asymmetries in the exotic nuclei. The first observation of the disappearance of the magic number ($N = 20$) was reported based on mass measurements of the neutron-rich nuclei ^{31,32}Na [2]. The experimental observation of the higher binding energies of these nuclei is a direct consequence of the large deformation [2]. A large deformation was also reported in the ground state of ^{32}Mg [3]. That large deformation was explained by considering intruder effects which suggest a clear vanishing of the shell gap between the sd and pf shells around $N = 20$ [4]. Later, in many neutron-rich nuclei around $N \sim 20$ and 28, large deviations in the nuclear structure from conventional shell models were observed [5–11]. These observation have been explained by considering tensor interactions, three-body interaction, etc. [12]. Large quadrupole collectivity in ^{32,34,36,38}Si [10] indicates a large fp-shell intruder component in its 2_1^+ excited state. Recently, a p-wave halo structure was also observed in ^{31}Ne [8] and ^{37}Mg [9]. In ^{33}Mg ($N = 21$), direct evidence of a multi-particle-hole ground-state configuration was reported,

*Corresponding author: ushasi.dattapramanik@saha.ac.in

which further suggests significant reduction and merging of the $N = 20,28$ shell gap [11]. These nuclei, in-spite of lying below the $N = 28$ shell closure, exhibit intrusion by the $\nu p_{3/2}$ orbital and thus contradict the normal shell model theory. Thus, the evolution of nuclear structure in this region leaves important footprints for a deeper understanding of the nucleon-nucleon interaction in neutron-rich nuclei. In this respect, ^{35}Al would be an interesting nucleus to explore. In 1979 Simons *et al.* [13] first identified the neutron-rich nucleus ^{35}Al produced in fragmentation of ^{40}Ar. Four decades later, except for some theoretical calculations [14–18], limited experimental information regarding the ground-state configuration of ^{35}Al is available. The ground-state information of a nucleus gives direct insight into the wave function. ^{35}Al (with $Z = 13$ and $N = 22$) lies between the shell closures $N = 20$ and 28. Experimental information about the ground states of nuclei (with odd-Z and $N = 22$) such as ^{37}P, ^{35}Al, and ^{33}Na has yet to be confirmed, in-spite of their identification in the late 1980s or 1990s. ^{35}Al, especially, has the least experimental information available in the literature. The β-decay branch of ^{35}Al was studied at ISOLDE [19,20] and GANIL [21]. Some deexcited γ rays of ^{35}Al have been reported [22,23]. The extracted $B(E2)$ value is 142(52) e^2fm^4 [22]. The measured mass [24,25] and β-decay half-life [26,27] at GANIL were in agreement with calculations using the WBMB interaction[4] with a complete $0\hbar\omega$ basis of states (i.e., 0p-0h neutron excitations across the $sd - fp$ shell gap). A one-neutron binding energy of 5.2 MeV can be interpreted as an enhanced pairing in a Hartree-Fock-Bogoliubov (HFB) calculation [29]. Recently, the inclusive measured cross section and momentum distribution of the fragment after one-neutron removal from ^{35}Al [28,29] showed occupancy of all orbitals (s, p, d, and f) across the shell gap between sd and pf. But to understand more deeply the nucleon-nucleon interaction, it is important to explore details of the different components of the wave function, which is possible via exclusive measurements. The γ-ray spectroscopy after Coulomb breakup is a direct probe for studying the ground-state configurations of loosely bound nuclei [30,31]. The study of exotic nuclei in and around the $N = 20$ and 28 shell closures via invariant mass analysis with γ-ray energy tagging can provide detailed components of the ground-state wave function [30], which will provide insightful information for further investigation of the nucleon-nucleon interaction in that region of nuclei. In this article the ground-state configuration of ^{35}Al obtained via Coulomb breakup will be reported. A comparison of the results with those obtained from a knockout reaction [29] and calculations with SDPF-M interaction will also be presented.

II. EXPERIMENT

A primary beam of ^{40}Ar (531A MeV), delivered by the Heavy Ion Synchrotron (SIS18) at GSI (Helmholtzzentrum für Schwerionenforschung GmbH), Darmstadt was fragmented, and a group of short lived radioactive isotopes ($^{29-31}$Na, $^{31-33}$Mg, ^{34,35}Al, etc.) with similar mass-to-charge ratio (A/Z between 2.55 to 2.85) were separated by the FRagment Separator (FRS) [32] according to their magnetic rigidity. The cocktail beam (as shown Fig. 1 in [33]) was transported to the

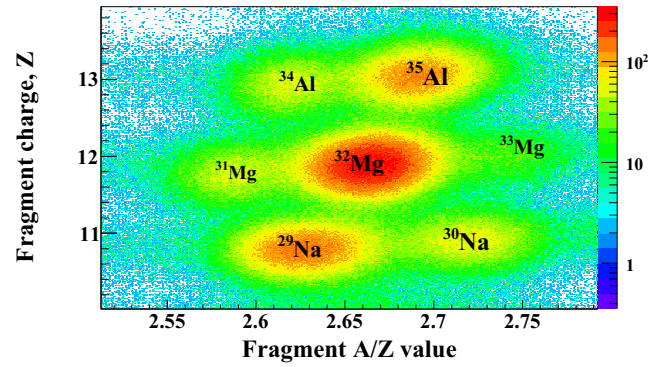

FIG. 1. Plot of charge against mass to charge ratio of outgoing reaction fragments.

experimental area where the LAND-FRS setup was employed for complete kinematic measurement. In that measurement, four-momenta of the projectile, fragments, and other decay products [i.e., fragments, neutron(s), and γ rays] after secondary reaction were measured. At the experimental area a fast plastic scintillator detector, POS, was placed before the secondary target for time-of-flight (TOF) measurement. The beam on the reaction target was adjusted using a plastic scintillator based active collimator detector. Unique identification of the secondary beam was made by energy loss measurement in a position-sensitive silicon pin diode (PSP) and time-of-flight measurements between two scintillator detectors (S8 and POS) before the reaction target. The reaction target was surrounded by eight double-sided silicon microstrip detector (DSSDs) form in a box-like structure. Four DSSDs were placed in-beam (two before and two after the reaction target) to track the projectiles and reaction fragments during secondary reactions. The reaction fragments were separated according to their magnetic rigidities by a large dipole magnet (ALADIN). The reaction fragments were tracked after ALADIN using two large scintillator fiber detectors (GFIs). The deflection angles of the charged fragments were obtained from tracking the reaction fragments using the two GFI detectors. The magnetic rigidity inside ALADIN was reconstructed from the measured deflection angle. The charge of the reaction fragment was measured from the energy-loss measurements in a large array of scintillator detectors with area of (2×2 m^2) (TFW) which consists of 32 paddles arranged orthogonally in two planes [34]. The mass of the reaction fragment was identified from the reconstructed magnetic rigidity and the time-of-flight (between POS and TFW) measurement of the reaction fragment. Figure 1 shows the outgoing mass-to-charge ratios of the reaction fragments against the charges, where the incoming cocktail beam was considered. The decayed neutrons from the excited projectiles were forward focused and were detected by the high efficiency Large Area Neutron Detector (LAND) [35] placed at 0° downstream of the reaction target. The one-neutron detection efficiency of LAND for neutrons with kinetic energy 400–450 MeV is ∼90%. The acceptance of one neutron produced after Coulomb breakup of ^{35}Al is almost 100% up to 3.5 MeV of the relative energy between the core and the neutron, and above that the acceptance decreases gradually. The γ rays from the deexcited projectile

and projectile-like fragments were detected by the 4π Crystal Ball detector. The Crystal Ball detector consists of 162 NaI(Tl) crystals arranged in a spherical shell with inner and outer radii of 25 and 45 cm, respectively. The efficiency of the Crystal Ball detector for γ rays of different energies has been obtained using a standard γ-ray source and through detailed GEANT4 simulation. The experimental results from radioactive calibration sources such as ^{22}Na and ^{60}Co were found to be in agreement (within 10%) with the simulated results. For more details about the setup, please see [11,33,34,36]. The secondary cocktail beam was bombarded on different reaction targets. Thick lead (2 g/cm^2) as a reaction target was used for studying electromagnetic excitation of the exotic nuclei (projectiles) and carbon (0.93 g/cm^2) as a reaction target was used for measuring the nuclear contribution. Data with the empty target were also taken to understand the background contribution arising from the reactions due to the detector materials. After the secondary reaction, the exotic nuclei can be excited. By measuring the four-momenta P_i of all the decay products, the excitation energy of the nucleus prior to decay can be reconstructed on an event-by-event basis by analyzing the invariant mass. The Coulomb dissociation cross section measured with the lead target (2 g/cm^2) was obtained after subtracting the nuclear contributions determined from the data obtained with a carbon target (0.93 g/cm^2). The scaling factor of the nuclear cross sections for a lead and a carbon target has been determined using the soft sphere model [37]. The background contribution from reactions induced by detectors materials was determined using the empty target data and has been subtracted with a proper normalizing factor from both the Pb and C target data.

III. COULOMB BREAKUP

The resulting data are analyzed on the basis of a direct-breakup model [30,38,39]. According to a direct-breakup model, a $^{A}X_{Z}$ nucleus is considered to consist of a core of $^{(A-1)}X_{Z}$ and a weakly bound valence nucleon. When such a loosely bound projectile at intermediate or high energy passes by a high-Z target, it may be excited by absorbing a virtual photon [39] and break up into a core and a neutron. In the breakup process, the valence nucleon occupying the single-particle bound state $|\psi_{n,l,j}\rangle$ is transported to the continuum state $|q\rangle$. The corresponding differential cross section $d\sigma/dE^*$ for dipole excitations decomposes into an incoherent sum of components $d\sigma(I_c^\pi)/dE^*$ corresponding to different core states with spin and parity I^π, populated after one-neutron removal. For each core state, the cross section furthermore decomposes into an incoherent sum over contributions from different angular momenta j of the valence neutron in its initial state [30]: The differential Coulomb dissociation cross section can be expressed as follows

$$\frac{d\sigma\left(I_c^\pi\right)}{dE^*} = \frac{16\pi^3}{9\hbar c} N_{E1}(E^*) \sum_j C^2 S\left(I_c^\pi, nlj\right) \times \sum_m \left|\left\langle q \left| (Ze/A) r Y_m^l \right| \psi_{nlj}(r) \right\rangle\right|^2. \quad (1)$$

$N_{E1}(E^*)$ is the number of equivalent virtual dipole photons of the target Coulomb field at an excitation energy E^*, which can be computed in a semiclassical approximation. Here, the final states $|q\rangle$ of the valence neutron can be approximated by a plane wave, and the single-particle initial states $|\psi_{n,l,j}\rangle$ can be derived from a Wood-Saxon potential.

The Coulomb dissociation cross section is very sensitive to the single-particle wave function $|\psi_{n,l,j}\rangle$, which in turn depends on the angular momentum (l) and the binding energy (S_n) of the valence neutron. Comparison of the experimental distribution of the Coulomb dissociation cross section with the theoretical one can provide direct insight into the angular momentum of the valence neutron and into its spectroscopic information [30]. The core state to which the valence neutron is attached can be identified by the characteristic γ rays.

IV. ANALYSIS AND RESULTS

The measured inclusive Coulomb dissociation cross section for $^{35}\mathrm{Al} \rightarrow {}^{34}\mathrm{Al} + n$ using a Pb target, integrated up to 5.0 MeV relative energy between core and the neutron, is 78(13) mb. Figure 2(a) shows the differential breakup cross section of ^{35}Al that breaks into ^{34}Al plus one neutron using lead (filled circles) and carbon targets (filled triangles). The differential CD cross section [open squares in Fig. 2(a)] was obtained after subtracting the nuclear part, measured using the carbon target with a scaling factor 1.8. The scaling factor corresponding to the ratio of the nuclear cross section in the lead target to that in the carbon target has been obtained using a soft-sphere model [37]. No resonance-like structure is observed in the CD spectra [Fig. 2(a)]. Figure 2(b) shows the sum-energy spectrum of γ rays decaying from the excited states of ^{34}Al after Coulomb breakup of ^{35}Al (filled circles), which is obtained in coincidence with ^{35}Al as an incoming beam, ^{34}Al as an outgoing fragment, and one neutron. The spectrum of the atomic background is obtained from measurement of the γ rays for an unreacted ^{35}Al beam on a Pb target and is represented by the short-dashed line (green online) in Fig. 2(b). The sum-energy spectrum of γ rays reflects the excited states populated after Coulomb breakup. The excited states of the odd-odd nuclei are very complicated. The density of states of such nuclei is high. Recently, a level scheme of excited states of ^{34}Al [40] was proposed from the β-decay studies of ^{34}Mg. With knowledge of the excited states of ^{34}Al from the literature, a detailed GEANT4 simulation was performed to understand the the sum-energy spectrum obtained from the present experiment. The detection efficiency of the sum-energy spectrum using the Crystal Ball spectrometer under experimental conditions was obtained. A prominent peak around 2.55 MeV is evident in the spectrum and is mainly deexcited by a cascade of two γ-ray transitions of 1.1 and 1.4 MeV. In addition to that excited state, after Coulomb breakup of ^{35}Al, three excited states were populated with small fractions, namely 2.0 and 1.46, and 1.048 MeV, as is evident from the sum-energy spectrum and the simulated spectrum. Recently, it was proposed from β-decay studies of ^{34}Mg [40] that the excited states around 1.04 and 1.46 MeV are above the isomeric states. In Fig. 2 (b) the solid line (black online) shows the spectrum obtained by summing the various

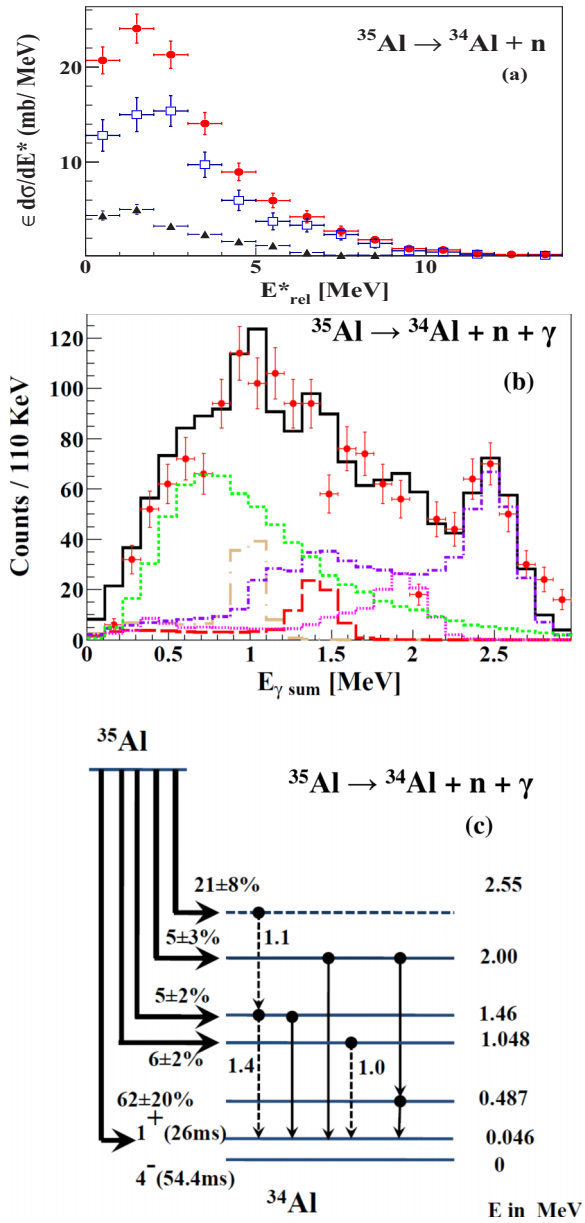

FIG. 2. (a) Inclusive differential CD cross section of ^{35}Al breaking up into a neutron and a ^{34}Al fragment, with respect to the relative energy (E_{rel}) between the core and the neutron. The filled circles and triangles represent the data using the Pb target and C target, respectively. The open squares represent the pure Coulomb part using the Pb target. (b) The experimental γ-ray sum-energy spectrum of ^{34}Al obtained after Coulomb breakup of ^{35}Al using the Pb target is represented by the filled circles (red online). The combination of a simulated γ-ray sum-energy spectrum of ^{34}Al and the atomic background is shown by the solid line (black online). The short-dashed line (green online) represents the atomic background obtained from the measurement of γ rays emitted from unreacted ^{35}Al at the secondary target. The simulated γ-ray sum-energy spectra decaying from the excited states with energy 1.04, 1.46, 2.0, and 2.55 MeV are represented by the dot–long-dashed line (brown online), long-dashed line (red online), dotted line (pink online), and dot–short-dashed line (violet online), respectively. (c) Partial level scheme of the ^{34}Al nucleus and the relative population of the states after Coulomb breakup of the ^{35}Al nucleus using the Pb target.

components of the simulated sum-energy spectra of the γ rays decaying from various excited states of the ^{34}Al nucleus and the experimental atomic background. In Fig. 2(b) the spectra with dot–short-dashed line (violet online), dotted line (pink online), long-dashed line (red online) and long–dashed-dotted line (brown online) represent the simulated spectra decaying from the 2.55, 2.0, 1.46, and 1.04 MeV excited states of ^{34}Al, respectively. To obtain the exclusive differential CD cross section for populating those excited states, the following ranges of the sum-energy of γ rays have been considered for gating conditions. The ranges considered for 1.04, 1.4, 2.0, and 2.55 MeV excited states were 0.7 to 1.2, 1.2 to 1.7, 1.7 to 2.2, and 2.2 to 2.9 MeV, respectively. The estimated detection efficiencies of the 1.04, 1.4, 2.0, and 2.55 MeV γ rays within the above energy ranges of the sum spectrum are 66(8)%, 57(7)%, 44(6)%, and 38(6)%, respectively. The combining correction factors for atomic background under the 1.04 and 1.4 MeV peaks and the feeding from higher energy levels to those energy levels are 80% and 84%, respectively. Similarly, for 2.0 and 2.55 MeV states the combined correction factors for the atomic background and feeding from other excited states are 70% and 13%, respectively. The excited-state contributions in $^{35}\mathrm{Al} \rightarrow {}^{34}\mathrm{Al} + n + \gamma$ are obtained from the γ-gated invariant mass spectra with corrections for the atomic background and the γ-detection efficiency of the Crystal Ball. Thus, after those corrections, the measured exclusive CD cross sections for populating the excited states of ^{34}Al at 1.04, 1.4, 2.0, and 2.55 MeV are 5(1), 4(1), 4(2), and 16(6) mb, respectively. Figure 2(c) shows the relative populations of different core states after Coulomb breakup of ^{35}Al. Figure 3 (filled squares) shows the exclusive differential CD spectra of ^{35}Al breaking up into a neutron and a ^{34}Al fragment in its ground state and/or isomeric state. The exclusive excited-state contributions are subtracted from the total inclusive differential Coulomb dissociation spectrum of ^{35}Al to obtain that exclusive differential CD spectrum which populated ^{34}Al in the ground state and/or isomeric state(s). The measured integrated CD cross section (integrated up to 5.0 MeV relative energy between the core and the neutron) for $^{35}\mathrm{Al} \rightarrow {}^{34}\mathrm{Al}_{\text{ground state and/or isomeric state}} + n$ is 48(13) mb. The exclusive data have been interpreted in the light of a direct breakup model in order to obtain information on the valence neutron occupying orbitals. The details of the analysis and interpretation of the results will be discussed in the next section.

V. DISCUSSION

To date, the ground-state spin and parity of ^{35}Al has not yet been experimentally confirmed. A ground-state spin of $5/2^+$ has been assumed from shell model calculations and the systematics of neighboring nuclei, considering the fact that the proton hole in the $d_{5/2}$ orbital is responsible for the ground-state spin and parity, while two valence neutrons in the $f_{7/2}$ orbital remain as spectators and do not contribute to the ground-state spin. This spin and parity has been used to explain the data of β decay [19] as well as the knockout experiment [29]. A number of excited states of this nucleus have been populated [23] by proton knockout, and the states

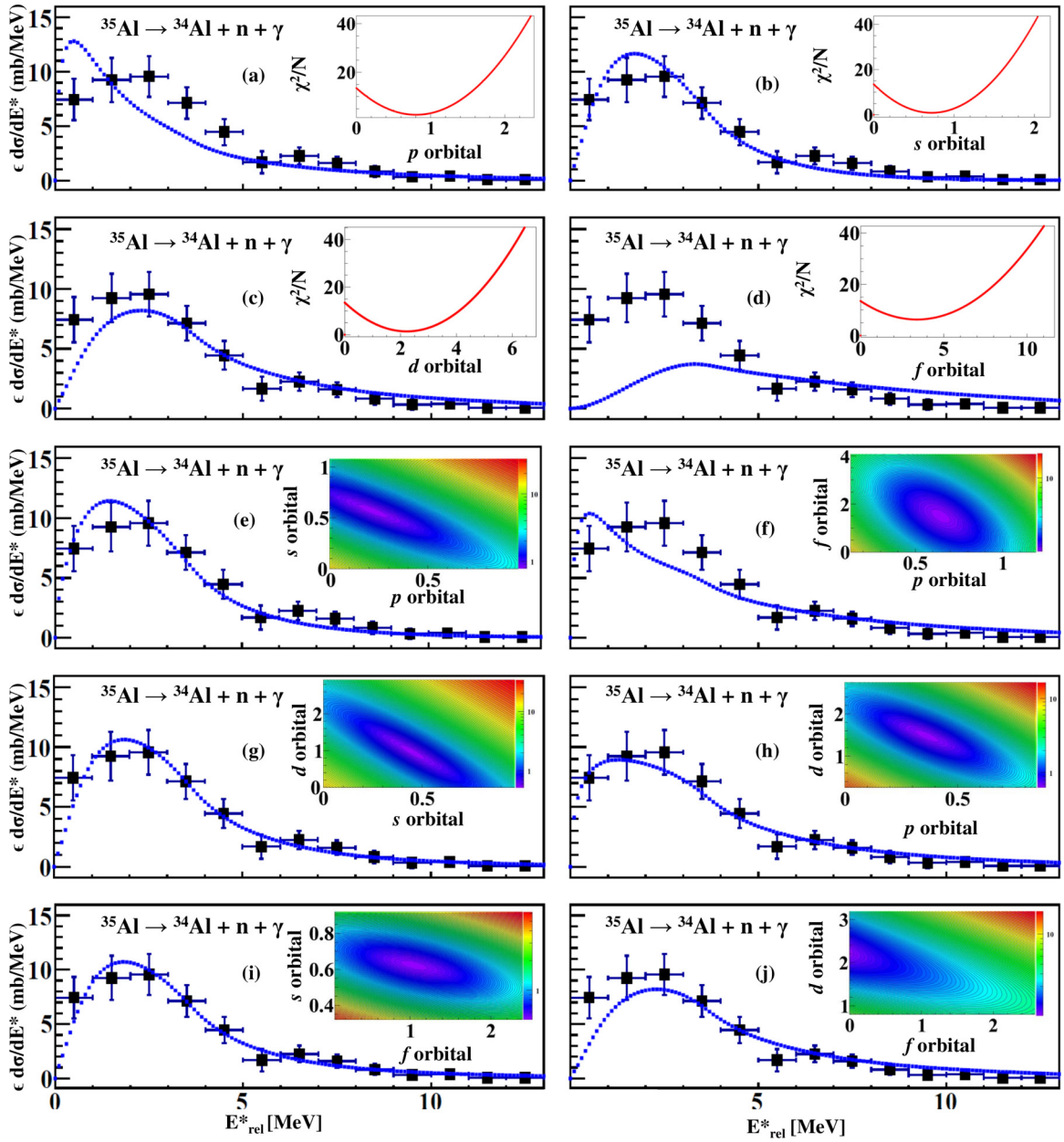

FIG. 3. Differential Coulomb dissociation cross section of ^{35}Al breaking up into a neutron and ^{34}Al in its ground state and/or isomeric state versus the relative energy (E_{rel}) between core and neutron. The dotted curves in (a), (b), (c), and (d) represent the calculation from the direct breakup model using the plane-wave approximation, where the valence neutron occupies p, s, d, and f orbitals, respectively. The corresponding inset panels show the corresponding one-dimensional χ^2 distributions. The dotted curves in (e), (f), (g), (h), (i), and (j) represent the calculation from the direct breakup model using the plane-wave approximation where the valence neutron occupies both p and s; p and f; s and d; p and d; f and s; and f and d orbitals, respectively. The inset panels show the corresponding two-dimensional χ^2 distributions. The experimental differential Coulomb dissociation cross sections are without the corrections for acceptance and efficiency of the neutron detector, LAND, while the calculated ones are folded with the response function of the experimental setup.

have been interpreted in the light of the SDPF-MU interaction [41]. According to the conventional shell model with neutron number $N = 22$, the valence neutron should occupy the $f_{7/2}$ orbital. In that situation, the Coulomb dissociation cross section of ^{35}Al for the one-neutron breakup channel would be around 4 mb with unit spectroscopic factor for the valence neutron. But the measured inclusive CD cross section of that nucleus, integrated up to 5.0 MeV relative energy between the core and the neutron using a Pb target, is 78(13) mb, and the measured CD cross section after subtracting the core excited-state contributions is 48(13) mb. Hence, the valence neutron cannot occupy the $f_{7/2}$ orbital alone. In order to understand the occupation of the orbital of the valence neutron, the exclusive differential CD cross section of the nucleus populating the core in the ground state and/or an isomeric state has been fitted with theoretical ones (using the

TABLE I. Various possible ground-state spins and parities of ^{35}Al, obtained from the present experimental data analysis and the corresponding major components of the ground-state configuration with the spectroscopic factors for the valence neutron occupying different orbitals

Possible ground-state spin and parity	Ground state configuration	The valence neutron occupying orbital	Spectroscopic factor for the neutron
$5/2^+$	$B_1\ ^{34}\mathrm{Al(g.s.};4^-)\otimes\nu_{p_{3/2}}$	p	0.36(0.09)
	$+B_2\ ^{34}\mathrm{Al(46\ keV};1^+)\otimes\nu_{d_{3/2}}$	d	1.47(0.22)
$1/2^+, 3/2^+$	$C_1\ ^{34}\mathrm{Al}(0;4^-)\otimes\nu_{f_{7/2}}$	f	1.03(0.43)
	$+\ C_2\ ^{34}\mathrm{Al(46\ keV};1^+)\otimes\nu_{s_{1/2}}$	s	0.62(0.07)
$1/2^+, 3/2^+$	$^{34}\mathrm{Al(46\ keV};1^+)\otimes\nu_{s_{1/2}}$	s	0.72(0.08)
$1/2^+, 3/2^+$	$C_1\ ^{34}\mathrm{Al(46\ keV};1^+)\otimes\nu_{s_{1/2}}$	s	0.45(0.07)
	$+\ C_2\ ^{34}\mathrm{Al(46\ keV};1^+)\otimes\nu_{d_{3/2}}$	d	0.94(0.22)

plane-wave approximation) corresponding to all possible valence neutron orbitals near the Fermi level. The theoretical curve has been convoluted with the experimental response function. The convoluted curve has been fitted with the experimental data using a chi-square minimization procedure. In ^{34}Al, an isomeric state [$T_{1/2} = 26(1)$ ms] at 0.46 MeV (1^+) has been reported [42]. Hence, it is necessary to consider the core as a system with an admixture of a 4^-[$T_{1/2} = 54.5(1)$ ms] [43] ground state with the 1^+ isomeric state [42]. Figures 3(a), 3(b), 3(c), and 3(d) show the histogram fitted with the convoluted direct breakup model calculation considering p, s, d, and f as the valence nucleon occupying orbitals, respectively. The inset panels in Figs. 3(a), 3(b), 3(c), and 3(d) show the corresponding one-dimensional χ^2 plotted against the spectroscopic factor of the valence neutron occupying that particular orbital. Figures 3(a), 3(c), and 3(d) show that the χ^2/N from the fitting is quite large (> 1). Hence, the valence neutron cannot occupy only the p, d, and f orbitals. If a valence neutron occupies a pure s orbital, the possible allowed configurations can be either $^{34}\mathrm{Al(g.s.};4^-)\otimes\nu_{s_{1/2}}$ or $^{34}\mathrm{Al(46\ keV};1^+)\otimes\nu_{s_{1/2}}$. The allowed spin and parity corresponding to the former and latter configurations are $(7/2;9/2)^-$ and $(1/2;3/2)^+$, respectively. Considering the β-decay experimental results for the allowed transition, it is expected that the parity of the ground state of ^{35}Al would be positive. If the ground-state parity of ^{35}Al is assumed to be positive, then $^{34}\mathrm{Al(46\ keV};1^+)\otimes\nu_{s_{1/2}}$ would be a possible configuration. The ground-state spin and parity could be either $1/2^+$ or $3/2^+$. Later, to explore the ground-state configuration in more detail, combinations of different orbitals were considered to fit the data. Figures 3(e), 3(f), 3(g), 3(h), 3(i), and 3(j) show the histograms fitted with an admixture of the convoluted direct breakup model calculation considering the valence neutron occupying both p and s; p and f; s and d; p and d; f and s; and f and d orbitals, respectively. The inset panels in Figs. 3(e), 3(f), 3(g), 3(h), 3(i), and 3(j) show the respective two-dimensional χ^2 plots. It is evident from the χ^2 plots of Figs. 3(e), 3(g), 3(h), and 3(i) that the possible orbitals for occupation of the valence nucleon are mixtures of p and s, s and d, p and d, and f and s orbitals. An admixture of the neutron orbitals corresponding to p and s waves can be interpreted as an admixture of $^{34}\mathrm{Al(g.s.};4^-)\otimes\nu_{p_{3/2}}$ and $^{34}\mathrm{Al(46\ keV};1^+)\otimes\nu_{s_{1/2}}$ configurations. When a mixture of these configurations is considered, a common spin and parity cannot be assigned to the ground state. So, this combination of the orbitals for occupation of the valence neutron can be discarded. Since β-decay data favor positive parity for the ground state, coupling of the valence neutron which occupies the s and d orbitals with the core in the isomeric state can be considered. An admixture of s and d wave neutrons can be interpreted as an admixture of $^{34}\mathrm{Al(46\ keV};1^+)\otimes\nu_{s_{1/2}}$ and $^{34}\mathrm{Al(46\ keV};1^+)\otimes\nu_{d_{3/2}}$ configurations. The tentative ground-state spin could be $(1/2)^+$ or $(3/2)^+$. When an admixture of p and d waves is considered, the allowed configurations are $^{34}\mathrm{Al(g.s.};4^-)\otimes\nu_{p_{3/2}}$ and $^{34}\mathrm{Al(46\ keV};1^+)\otimes\nu_{d_{3/2}}$. But the possible ground-state spin and parity considering a combination of configurations could be $5/2^+$. In an admixture of f and s waves, conservation of parity allows an admixture of the $^{34}\mathrm{Al(550\ keV};1^+)\otimes\nu s_{1/2}$ and $^{34}\mathrm{Al(g.s.};4^-)\otimes\nu_{f_{7/2}}$ configurations. The possible tentative spin and parity could be either $(1/2)^+$ or $(3/2)^+$. Thus, the possible ground-state spin and parity of ^{35}Al could be tentatively, $1/2^+$ or $3/2^+$, or $5/2^+$ according to the present experimental data analysis. Table I shows the possible tentative ground-state spin with configurations which have been obtained from the present experimental data analysis. Thus if $5/2^+$ can be considered as a ground-state spin, then the valence neutron can occupy the p and d orbitals coupled with the core in the ground state and isomeric state respectively. It is quite important to compare the unknown and new results obtained from one method of experiment with that from another complementary method. With that view point, a comparison of the measured spectroscopic factor with knockout measurements [29] has been performed. This is shown in Fig. 4. The knockout measurement [29] was performed at GSI, Darmstadt. The inclusive momentum distribution of ^{34}Al, obtained after one-neutron knockout from ^{35}Al, was measured by FRS and compared with the calculation in the framework of the eikonal approximation. The spectroscopic factors for the valence neutron, occupying the s, d, and p orbitals, in the ground state of ^{35}Al [29] are represented by a filled circle, triangle, and square, respectively. The results from the present experimental work are represented by open symbols. The spectroscopic factors of the valence neutron in the p and d orbitals were obtained by fitting exclusive differential CD cross sections,

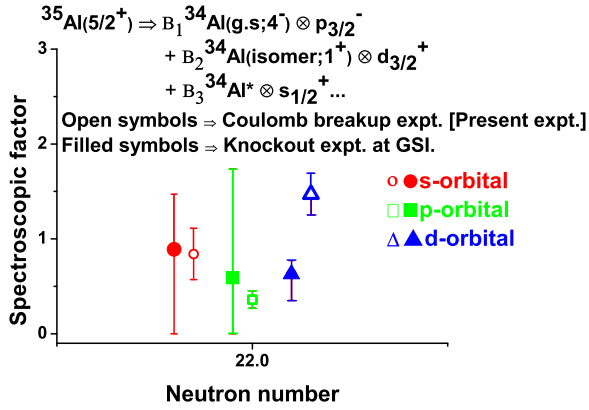

FIG. 4. The comparison of the spectroscopic factors of the valence neutron in the the ground state of ^{35}Al $(5/2^+)$, obtained from the present measurement with that from a knockout measurement [29]. The spectroscopic factors for the valence neutron, occupying the s, d, and p orbitals, in the ground state of ^{35}Al [29] are represented using a circle, triangle, and square, respectively. The results from the present measurement are represented by open symbols while the filled ones represent the knockout measurement [29].

but the spectroscopic factor for the s orbital was obtained from the inclusive measured data with consideration of the p and the d components, obtained from the exclusive measurement data. It is obvious from the figure that the spectroscopic factor for low l orbitals, i.e., the s and the p, within errors, are in close agreement. The errors mentioned in this article corresponding to the present measurement are 1σ (68% confidence limit). But the situation for the d component is different and the spectroscopic factor is in agreement in two methods, considering error, with a 99% confidence limit. To understand further details, the measured spectroscopic factors have been compared with the shell model calculation using the original SDPF-M interaction [44,45]. The calculation is performed with the conventional shell model, where the model space has been truncated so that the neutrons are allowed to occupy up to $4p$-$3h$ configurations for positive parity and up to $5p$-$4h$ configurations for negative parity. Thus, the shell gaps adopted are the same as in the paper [44], and the calculation has been performed considering the ground state as $1/2^+$, $3/2^+$, and $5/2^+$. Table II shows a comparison of the spectroscopic factors obtained from the present Coulomb breakup experiment, previous knockout measurements [29], and theoretical calculations using the SDPF-M interaction for the ground-state spin and parity of ^{35}Al as $5/2^+$. From Table II, it is evident that the spectroscopic factor for the p orbital obtained from the present Coulomb breakup measurement is closer to the calculation than that obtained from the knockout measurement [29]. In contrast, the spectroscopic factor for the d orbital is in closer agreement with that obtained from the knockout measurement. In the calculation, a number of core excited states with energy below 1.0 MeV have been predicted which are coupled with the neutron in the d orbital. Those details are found in Table II. It may be noted that the SDPF-M calculation predicts occupation of the valence neutron in the $f_{7/2}$ orbital with spectroscopic factor (0.6). Moreover, it has been observed that the spectroscopic factors for the p and the d orbitals, obtained from the present experimental data, are higher in value compared to those predicted by the SDPF-M calculation. Considering those facts, the data have been fitted with the direct breakup model calculation with partial occupation in the f orbital along with other orbital(s). A meaningful information can be obtained by constraining the spectroscopic factor for the d orbital. The lower limit of the fitted spectroscopic factor of the d orbital, considering errors with 99.9% confidence limit, is 1.0 (see Table II). After constraining a maximum limit of the spectroscopic factor of the d orbital to 1.0, the spectroscopic factors for the p and f orbitals, obtained from fitting of the data, are 0.48(0.08) and $0.24^{+0.42}_{-0.24}$, respectively. In conclusion, the enhanced Coulomb dissociation cross section of ^{35}Al clearly suggests that the neutron may occupy orbitals which are a combination of sd and pf orbitals. The experimental data have been compared with the SDPF-M calculation and the comparison favors the ground-state spin and parity $5/2^+$. Since the neutron may occupy orbitals which are a combination of the sd and pf shells, one is able to conclude that there is a narrower shell gap between these shells, i.e., at the $N = 20$ and 28 magic numbers. Similar observations have been reported in ^{33}Mg [11]. In contrast, a similar measurement shows that the valence

TABLE II. Measured CD cross sections of the ^{35}Al nucleus integrated up to 5.0 MeV relative energy between the core and the neutron, and the spectroscopic factors for the valence neutron in the ground state of ^{35}Al $(5/2^+)$ coupled with the various core states, obtained from calculations (SDPF-M), the present measurement, and a previously reported knockout measurement [29].

Core state		Neutron	Coulomb dissociation		Spectroscopic factor		
Experiment	SDPF-M [44,45]	orbital	(CD) cross section (mb)		Shell model	Experiment	
I^π (E (MeV))	I^π (E (MeV))		Direct breakup	Experiment CD	SDPF-M	CD	Knockout [29]
$4^-(0.0)$	$4^-(0.0)$	$p_{3/2}$	47		0.1	0.36(0.09)	$0.59^{+1.15}_{-0.59}$
	$3^-(0.29)$				0.09		
				48(13)			
$1^+_{\text{isomer}}(0.046)$	$1^+(0.38)$	$d_{3/2}$	16		0.22	1.47(0.22)	$0.63^{+0.14}_{-0.28}$
	$4^+(0.6)$				0.7		
	$2^+(0.82)$				0.36		

neutron in the ground state of neutron-rich nuclei ^{29,30}Na is mainly occupying the d orbital [33]. Future experiments with different complementary methods using a radioactive ion beam with higher statistics may provide insightful information about the structure of this interesting neutron-rich exotic nucleus.

VI. SUMMARY

Coulomb breakup of the neutron-rich nucleus ^{35}Al has been studied at a relativistic energy 403A MeV. Four-momenta of the projectile, fragment, and neutron after reaction were measured and the excitation energy of the nucleus prior to the decay has been reconstructed by analyzing the invariant mass. The measured inclusive differential CD cross section (integrated up to 5.0 MeV relative energy) for $^{35}\mathrm{Al} \rightarrow {}^{34}\mathrm{Al} + n$ using a Pb target is 78(13) mb. The inclusive and exclusive data have been interpreted in the light of the direct breakup model and suggest that the data cannot be explained by pure occupation of the valence neutron in the $f_{7/2}$ orbital, as predicted by the conventional shell model. The possible ground-state spin and parity of ^{35}Al is either $1/2^+$ or $3/2^+$ or $5/2^+$ according to the present experimental data analysis. If the ground-state spin is $1/2^+$ or $3/2^+$, then the major ground-state configuration could be $^{34}\mathrm{Al(g.s.;}4^-) \otimes \nu_{f_{7/2}}$ and $^{34}\mathrm{Al(46\ keV;}1^+) \otimes \nu_{s_{1/2}}$. However, consideration of the shell model calculation and Coulomb breakup results in the light of the direct breakup model favors $5/2^+$ as the ground-state spin and parity. The major components of the ground-state configuration, with consideration of that spin and parity, are $^{34}\mathrm{Al(g.s.;}4^-) \otimes \nu_{p_{3/2}}$ and $^{34}\mathrm{Al(46\ keV;}1^+) \otimes \nu_{d_{3/2}}$. The obtained spectroscopic factors for the occupied valence neutron orbitals have been compared with a SDPF-M shell model calculation and those obtained from the knockout measurement [29]. Since the neutron may occupy orbitals which are a combination of the sd shell and pf shells, one may conclude the existence of a narrower shell gap between the sd and pf shells at the $N = 20,28$ magic numbers.

ACKNOWLEDGMENTS

The authors are thankful to the accelerator staff of GSI for their support during the experiment. The authors are also thankful to Prof. Ajit Mahanty, SINP, Kolkata for critically reviewing the manuscript and providing valuable suggestions. Author Ushasi Datta gratefully acknowledges the Alexander von Humboldt (AvH) foundation for financial support to execute the project of exploring disappearance of the "magic numbers" in exotic nuclei. This work is a part of that Project. This work has been partially funded by the XIth plan, SEND Project (PIN:11-R&D-SIN-5.11-0400), DAE, Government of India.

[1] M. G. Mayer, Phys. Rev. **75**, 1969 (1949); O. Haxel, *ibid.* **75**, 1766 (1949).
[2] C. Thibault *et al.*, Phys. Rev. C **12**, 644 (1975).
[3] T. Motobayashi *et al.*, Phys. Lett. B **346**, 9 (1995).
[4] E. K. Warburton, J. A. Becker, and B. A. Brown, Phys. Rev. C **41**, 1147 (1990).
[5] R. Klapisch *et al.*, Phys. Rev. Lett. **23**, 652 (1969).
[6] B. Bastin, S. Grevy, D. Sohler, O. Sorlin, Z. Dombradi, N. L. Achouri, J. C. Angelique, F. Azaiez, D. Baiborodin, R. Borcea, C. Bourgeois, A. Buta, A. Burger, R. Chapman, J. C. Dalouzy, Z. Dlouhy, A. Drouard, Z. Elekes, S. Franchoo, S. Iacob, B. Laurent, M. Lazar, X. Liang, E. Lienard, J. Mrazek, L. Nalpas, F. Negoita, N. A. Orr, Y. Penionzhkevich, Z. Podolyak, F. Pougheon, P. Roussel-Chomaz, M. G. Saint-Laurent, M. Stanoiu, I. Stefan, F. Nowacki, and A. Poves, Phys. Rev. Lett. **99**, 022503 (2007).
[7] S. Takeuchi, M. Matsushita, N. Aoi, P. Doornenbal, K. Li, T. Motobayashi, H. Scheit, D. Steppenbeck, H. Wang, H. Baba, D. Bazin, L. Caceres, H. Crawford, P. Fallon, R. Gernhauser, J. Gibelin, S. Go, S. Grevy, C. Hinke, C. R. Hoffman, R. Hughes, E. Ideguchi, D. Jenkins, N. Kobayashi, Y. Kondo, R. Krucken, T. LeBleis, J. Lee, G. Lee, A. Matta, S. Michimasa, T. Nakamura, S. Ota, M. Petri, T. Sako, H. Sakurai, S. Shimoura, K. Steiger, K. Takahashi, M. Takechi, Y. Togano, R. Winkler, and K. Yoneda, Phys. Rev. Lett. **109**, 182501 (2012).
[8] T. Nakamura, N. Kobayashi, Y. Kondo, Y. Satou, J. A. Tostevin, Y. Utsuno, N. Aoi, H. Baba, N. Fukuda, J. Gibelin, N. Inabe, M. Ishihara, D. Kameda, T. Kubo, T. Motobayashi, T. Ohnishi, N. A. Orr, H. Otsu, T. Otsuka, H. Sakurai, T. Sumikama, H. Takeda, E. Takeshita, M. Takechi, S. Takeuchi, Y. Togano, and K. Yoneda, Phys. Rev. Lett. **112**, 142501 (2014).
[9] N. Kobayashi, T. Nakamura, Y. Kondo, J. A. Tostevin, Y. Utsuno, N. Aoi, H. Baba, R. Barthelemy, M. A. Famiano, N. Fukuda, N. Inabe, M. Ishihara, R. Kanungo, S. Kim, T. Kubo, G. S. Lee, H. S. Lee, M. Matsushita, T. Motobayashi, T. Ohnishi, N. A. Orr, H. Otsu, T. Otsuka, T. Sako, H. Sakurai, Y. Satou, T. Sumikama, H. Takeda, S. Takeuchi, R. Tanaka, Y. Togano, and K. Yoneda, Phys. Rev. Lett. **112**, 242501 (2014).
[10] R. W. Ibbotson, T. Glasmacher, B. A. Brown, L. Chen, M. J. Chromik, P. D. Cottle, M. Fauerbach, K. W. Kemper, D. J. Morrissey, H. Scheit, and M. Thoennessen, Phys. Rev. Lett. **80**, 2081 (1998).
[11] U. Datta *et al.*, Phys. Rev. C **94**, 034304 (2016).
[12] T. Otsuka, R. Fujimoto, Y. Utsuno, B. A. Brown, M. Honma, and T. Mizusaki, Phys. Rev. Lett. **87**, 082502 (2001); T. Otsuka, T. Suzuki, R. Fujimoto, H. Grawe, Y. Akaishi, *ibid.* **95**, 232502 (2005); T. Otsuka, T. Suzuki, M. Honma, Y. Utsuno, N. Tsunoda, K. Tsukiyama, M. Hjorth-Jensen, *ibid.* **104**, 012501 (2010).
[13] T. J. M. Symons, Y. P. Viyogi, G. D. Westfall, P. Doll, D. E. Greiner, H. Faraggi, P. J. Lindstrom, D. K. Scott, H. J. Crawford, and C. McParland, Phys. Rev. Lett. **42**, 40 (1979).
[14] P. Moller *et al.*, At. Data Nucl. Data Tables **26**, 165 (1981).
[15] A. Poves *et al.*, Nucl. Phys. A **571**, 221 (1994).
[16] M. Kimura, Int. J. Mod. Phys. E **20**, 893 (2011).
[17] M. K. Sharma *et al.*, Int. J. Mod. Phys. E **22**, 1350005 (2013).
[18] E. Caurier, F. Nowacki, and A. Poves, Phys. Rev. C **90**, 014302 (2014).

[19] S. Nummela, P. Baumann, E. Caurier, P. Dessagne, A. Jokinen, A. Knipper, G. L. Scornet, C. Miehé, F. Nowacki, M. Oinonen, Z. Radivojevic, M. Ramdhane, G. Walter, and J. Aysto (ISOLDE Collaboration), Phys. Rev. C **63**, 044316 (2001).
[20] S. Nummela *et al.*, Nucl. Phys. A **701**, 410C (2002).
[21] C. Timis *et al.*, J. Phys. G **31**, S1965 (2005).
[22] R. W. Ibbotson, T. Glasmacher, P. F. Mantica, and H. Scheit, Phys. Rev. C **59**, 642 (1999).
[23] S. R. Stroberg, A. Gade, J. A. Tostevin, V. M. Bader, T. Baugher, D. Bazin, J. S. Berryman, B. A. Brown, C. M. Campbell, K. W. Kemper, C. Langer, E. Lunderberg, A. Lemasson, S. Noji, F. Recchia, C. Walz, D. Weisshaar, and S. J. Williams, Phys. Rev. C **90**, 034301 (2014).
[24] A. Gillibert *et al.*, Phys. Lett. B **192**, 39 (1987).
[25] N. A. Orr *et al.*, Phys. Lett. B **258**, 29 (1991).
[26] A. C. Mueller *et al.*, Z. Phys. A **330**, 63 (1988).
[27] M. Lewitowicz *et al.*, Nucl. Phys. A **496**, 477 (1989).
[28] C. Rodriguez-Tajes *et al.*, Phys. Rev. C **82**, 024305 (2010).
[29] C. Nociforo, A. Prochazka, R. Kanungo, T. Aumann, D. Boutin, D. Cortina-Gil, B. Davids, M. Diakaki, F. Farinon, H. Geissel, R. Gernhauser, R. Janik, B. Jonson, B. Kindler, R. Knobel, R. Krucken, N. Kurz, M. Lantz, H. Lenske, Y. A. Litvinov, B. Lommel, K. Mahata, P. Maierbeck, A. Musumarra, T. Nilsson, C. Perro, C. Scheidenberger, B. Sitar, P. Strmen, B. Sun, I. Szarka, I. Tanihata, H. Weick, and M. Winkler, Phys. Rev. C **85**, 044312 (2012).
[30] U. D. Pramanik *et al.*, Phys. Lett. B **551**, 63 (2003).
[31] U. D. Pramanik, Prog. Part. Nucl. Phys. **59**, 183 (2007).
[32] H. Geissel *et al.*, Nucl. Instrum. Methods B **70**, 286 (1992).
[33] A. Rahaman *et al.*, J. Phys. G **44**, 045101 (2017).
[34] A. Rahaman *et al.*, EPJ web of conf. **66**, 02087 (2014).
[35] T. Blaich *et al.*, Nucl. Instrum. Methods A **314**, 136 (1992).
[36] C. Caesar *et al.*, Phys. Rev. C **88**, 034313 (2013).
[37] C. J. Benesh, B. C. Cook, and J. P. Vary, Phys. Rev. C **40**, 1198 (1989).
[38] T. Nakamura *et al.*, Phys. Lett. B **331**, 296 (1994).
[39] C. A. Bertulani and G. Baur, Phys. Rep. **163**, 299 (1988).
[40] R. Licâ, F. Rotaru, M. J. G. Borge, S. Grevy, F. Negoita, A. Poves, O. Sorlin, A. N. Andreyev, R. Borcea, C. Costache, H. DeWitte, L. M. Fraile, P. T. Greenlees, M. Huyse, A. Ionescu, S. Kisyov, J. Konki, I. Lazarus, M. Madurga, N. Marginean, R. Marginean, C. Mihai, R. E. Mihai, A. Negret, R. D. Page, J. Pakarinen, S. Pascu, V. Pucknell, P. Rahkila, E. Rapisarda, A. Serban, C. O. Sotty, L. Stan, M. Stanoiu, O. Tengblad, A. Turturica, P. Van Duppen, R. Wadsworth, and N. Warr, Phys. Rev. C **95**, 021301(R) (2017).
[41] Y. Utsuno, T. Otsuka, B. A. Brown, M. Honma, T. Mizusaki, and N. Shimizu, Phys. Rev. C **86**, 051301 (2012).
[42] F. Rotaru, F. Negoita, S. Grevy, J. Mrazek, S. Lukyanov, F. Nowacki, A. Poves, O. Sorlin, C. Borcea, R. Borcea, A. Buta, L. Caceres, S. Calinescu, R. Chevrier, Z. Dombradi, J. M. Daugas, D. Lebhertz, Y. Penionzhkevich, C. Petrone, D. Sohler, M. Stanoiu, and J. C. Thomas, Phys. Rev. Lett. **109**, 092503 (2012).
[43] P. Himpe *et al.*, Phys. Lett. B **658**, 203 (2008).
[44] Y. Utsuno, T. Otsuka, T. Mizusaki, and M. Honma, Phys. Rev. C **60**, 054315 (1999).
[45] Y. Utsuno, T. Otsuka, T. Mizusaki, and M. Honma, Phys. Rev. C **64**, 011301 (2001); **70**, 044307 (2004).